Proceedings of the Institution of Civil Engineers
Structures and Buildings 162
February 2009 Issue SB1
Pages 45–56
doi: 10.1680/stbu.2009.162.1.45

Paper 700058
Received 17/10/2007
Accepted 15/10/2008

Keywords: beams & girders/ concrete structures/strength & testing of materials

Yi Chen
Loads Engineer, Garrad Hassan & Partner Ltd, St Vincent's Works, Bristol, UK

Ian M. May
Professor of Civil Engineering, School of the Built Environment, Heriot Watt University, Edinburgh, UK

ice
Institution of Civil Engineers

Reinforced concrete members under drop-weight impacts

Y. Chen MSc, PhD and I. M. May MSc, PhD, CEng, FICE, FIStructE

This paper describes a series of experimental studies to investigate the high-mass, low-velocity impact behaviour of reinforced concrete members including beams and slabs, and to provide high-quality input data and results to validate numerical modelling. Fourteen 2·7 m and four 1·5 m span beams, four 0·8 m square 76 mm thick and two 2·3 m square 150 mm thick slabs were tested under impact loads using a drop-weight facility. Measurements included transient impact loads, accelerations and strains in the steel reinforcement. Additionally the impact events were recorded using a high-speed video camera operated at up to 4500 frames per second. For the beam tests, the local failure pattern of a beam under the impact zone was examined by correlating the images of development of cracks, spalling and scabbing with the impact load history. For the slab tests, the imposed energy on a slab was compared with the minimum energy causing the slab to scab, which was predicted using empirical formulae. The investigations enabled a better understanding of the behaviour of reinforced concrete members subject to impact loads.

1. INTRODUCTION

Reinforced concrete structures might be exposed sometime in their lives to some extreme dynamic loading conditions owing to impacts. Typical examples include transportation structures subjected to vehicle crash impact, marine and offshore structures exposed to ice impact or dropped object impact from passing ships, protective structures under projectile or aircraft impact and civil structures impacted by tornado-borne debris. In recent years the assessment of the performance and vulnerability of concrete reinforced structures under an impact load has become more important.[1] Increasingly engineers are resorting to numerical models to carry out designs, assessments and safety checks, and there is a requirement for high-quality data from physical tests to assist in validation of these models.

When subjected to an impact load, structural members can behave differently compared with those under a static load, owing to the transient and usually localised pattern of impact loading. The dynamic properties of materials can also be different to those under static loading. Investigations[2–4] have shown that both concrete and steel are stress/strain rate sensitive: both the tensile and compressive strengths and Young's modulus can increase if there is an increase in the stress/strain rate.

There have been a number of studies of impact on reinforced concrete members, in particular drop-weight impact tests on reinforced and prestressed concrete beams. Kishi and his co-workers conducted drop-weight impact tests in which a beam failed in either a bending or shear failure mode.[5,6] The impact forces, reactions and deflections of the beams were measured, and the absorbed energy of a beam was determined using the reaction forces at the supports and residual deflection of the beam at mid-span. Empirical design formulae were then proposed based on the static bending or shear capacity of a beam and required residual displacement. Given the dynamic nature of impact-loaded reinforced concrete structures, a degree of scatter was found between the test results and the predictions from the proposed design formulae.

A comprehensive series of tests on single-span reinforced concrete beams, using a drop-weight impact facility, was conducted by Hughes and Speirs.[7] The impacts were imposed to the top of the beams at mid-span through a plywood or steel pad, in order that the stiffness of the impact zone could be varied. In the majority of the tests the beam failed in a flexural mode, with flexural cracks at the bottom of the beam concentrated towards the mid-span, and at the top of the beam at 1/5 and 5/6 span. Diagonal cracks were observed in the impact zone and shear cracks at 1/3 and 2/3 span on the beam in some of the tests. It was found that the stiffness of the impact zone, which was a function of the impactor, the pad and the local stiffness of the beam, had a more significant influence than the support conditions on the response of the beam and that high vibration modes were more likely to be excited as the impact zone became stiffer. A theoretical analysis, based on an elastic vibration model of beams, was used to determine impact force–time history and limits of beam displacement. While the analysis gave a reasonable predication of impact forces and extents of beam displacement, it was concluded that a more accurate analysis would be beneficial in order to account for cracking, crushing, yielding of the reinforcement and strain rate effects, if there are any.

Agardh *et al.*[8] investigated the impact resistance of high-strength concrete reinforced concrete beams. Strain gauges attached to the surface of reinforcing bars were used to measure the reinforcement strains. A strain rate of 102/s in the reinforcement was reported to have been recorded. Strain gauges installed in this way are considered to affect the bond between the bars and surrounding concrete. It is therefore

difficult for the gauges to provide accurate results where a crack occurs and they are easily damaged, as occurred with some of the gauges in Agardh's tests.

A vast number of investigations into reinforced concrete slabs under impacts have also been carried out.[9,10] The effects of various parameters were studied, including size of slabs, ratio of reinforcement, shape of impactors and impact velocities. Both drop-weight and hydraulic testing machines were used to test slabs under low-velocity impacts (up to 10 m/s).[11,12] The failure patterns found in the tests included spalling, penetration, scabbing, perforation and shear plugs.[13]

Owing to the complexity of the impact behaviour of reinforced concrete structures, impacted structural members have been generally evaluated using empirical formulae to provide estimates on the extent of any impact damage, such as penetration depth, the possibility of scabbing or perforation for slabs[14] and the load capacity for beam.[5,6] With the advancement of modern computing facilities and finite-element theories, more details of the dynamic response of structural members can be accounted for.[15–18] Recently, computational techniques based on combined continuum/discontinuum (finite/discrete element) methods have been developed for simulating the impact behaviour of reinforced concrete beams,[19] especially within the nonlinear range when extensive cracking of the concrete can take place in conjunction with yielding of the steel reinforcement.

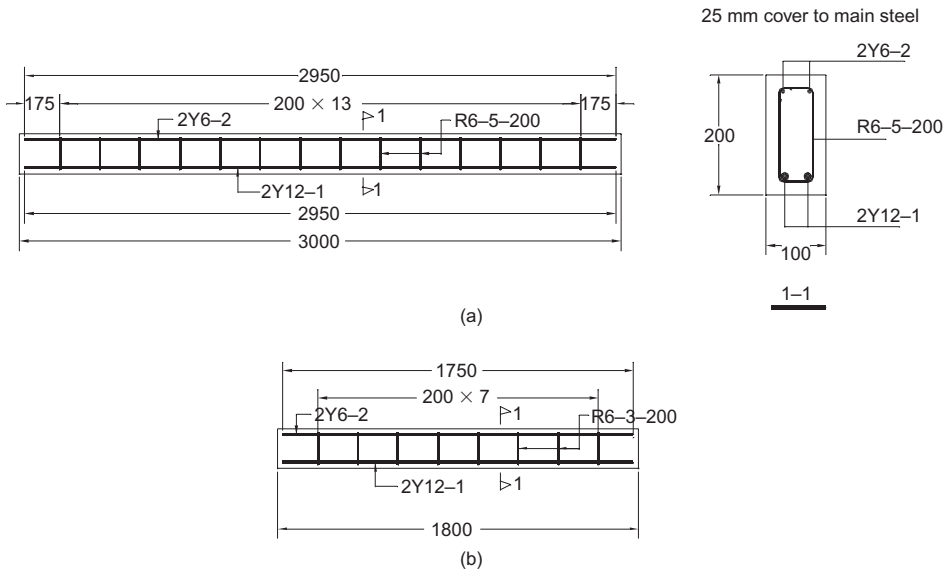

Figure 1. Reinforcement details for: (a) 3·0 m beam; (b) 1·8 m beams (dimensions in mm)

Group no.	Test no.	L_{sp}: m	f_{cu}: N/mm^2	f_t^3: N/mm^2	Support	Impactor	Impact interface
A1	1	2·7	49·2	1·71	Pin-ended	Hemispherical	12 mm plywood
	2	2·7	49·2	1·71	Pin-ended	Hemispherical	12 mm plywood
	3	2·7	49·2	1·71	Pin-ended	Hemispherical	12 mm plywood
	4	2·7	49·2	1·71	Pin-ended	Hemispherical	12 mm plywood
	5	2·7	45·8	1·86	Pin-ended	Hemispherical	12 mm plywood
	6	2·7	45·8	1·86	Pin-ended	Hemispherical	12 mm plywood
A1*	7	2·7	33·6	1·53	pin-ended	Hemispherical	12 mm plywood
A2	8	2·7	45·8	1·86	Simply supported	Hemispherical	12 mm plywood
	9	2·7	42·8	1·64	Simply supported	Hemispherical	12 mm plywood
A3	10	1·5	35·6	1·73	Pin-ended	Hemispherical	12 mm plywood
B1	11	2·7	33·6	1·53	Pin-ended	Hemispherical	Direct contact
	12	2·7	33·6	1·53	Pin-ended	Hemispherical	Direct contact
B1*	13	2·7	45·8	1·86	Pin-ended	Hemispherical	Direct contact
B2	14	1·5	35·6	1·73	Pin-ended	Hemispherical	Direct contact
	15	1·5	35·6	1·73	Pin-ended	Hemispherical	Direct contact
B3	16	2·7	42·8	1·64	Pin-ended	Flat	Direct contact
B3*	17	2·7	33·6	1·53	Pin-ended	Flat	Direct contact
B4	18	1·5	35·6	1·73	Pin-ended	Flat	Direct contact

Notes:
All tests were conducted under a drop-weight of 98·7 kg with an impact velocity of 7·3 m/s.
L_{sp} is the distance (span) between the centres of 200 mm long supports at two ends.
f_t, the tensile strength of concrete, is based on the results of the splitting test of cylinders.
* Denotes the repeated test in which all conditions were the same as the test without an asterisk except concrete with different strength.
Properties of high-yield steel: Young's modulus—190 kN/mm^2, 0·2% proof tensile strength—510 N/mm^2, ultimate tensile strength—600 N/mm^2.
Tension steel percentage, 0·85%.

Table 1. Details of impact beam tests

The experimental work described in the current paper has been motivated by a lack of high-quality test results that has hampered the development and appraisal of such computational simulation techniques as mentioned above. The objective was to provide both the necessary input data for computation and results with which to appraise the numerical predictions. The strategy has been devised as that under the assumption that, by undertaking a controlled series of experimental studies, the final extent of the impact damage to the specimens together with the development of the failure mechanism in time can be recorded. The latter included monitoring the transient impact force, deformations/accelerations, strains and the progress of cracking, spalling and scabbing during the tests. The findings from the study should

Slab no.	Striker mass: kg	Impactor	Impact velocity: m/s	Steel ratio: %	Concrete cube strength: N/mm^2	Concrete tensile strength: N/mm^2
1	98·7	Hemispherical	6·5	0·6	60·0	4·06
2	98·7	Hemispherical	6·5	0·6	60·0	4·06
3	98·7	Flat	6·5	0·6	60·0	4·06
4	98·7	Hemispherical	8·0	1·1	60·0	4·06
5	196·7	Hemispherical	8·7	0·5	47·3	2·93
6	382·0	Hemispherical	8·3	0·5	55·7	2·93

Table 2. Details of slab tests

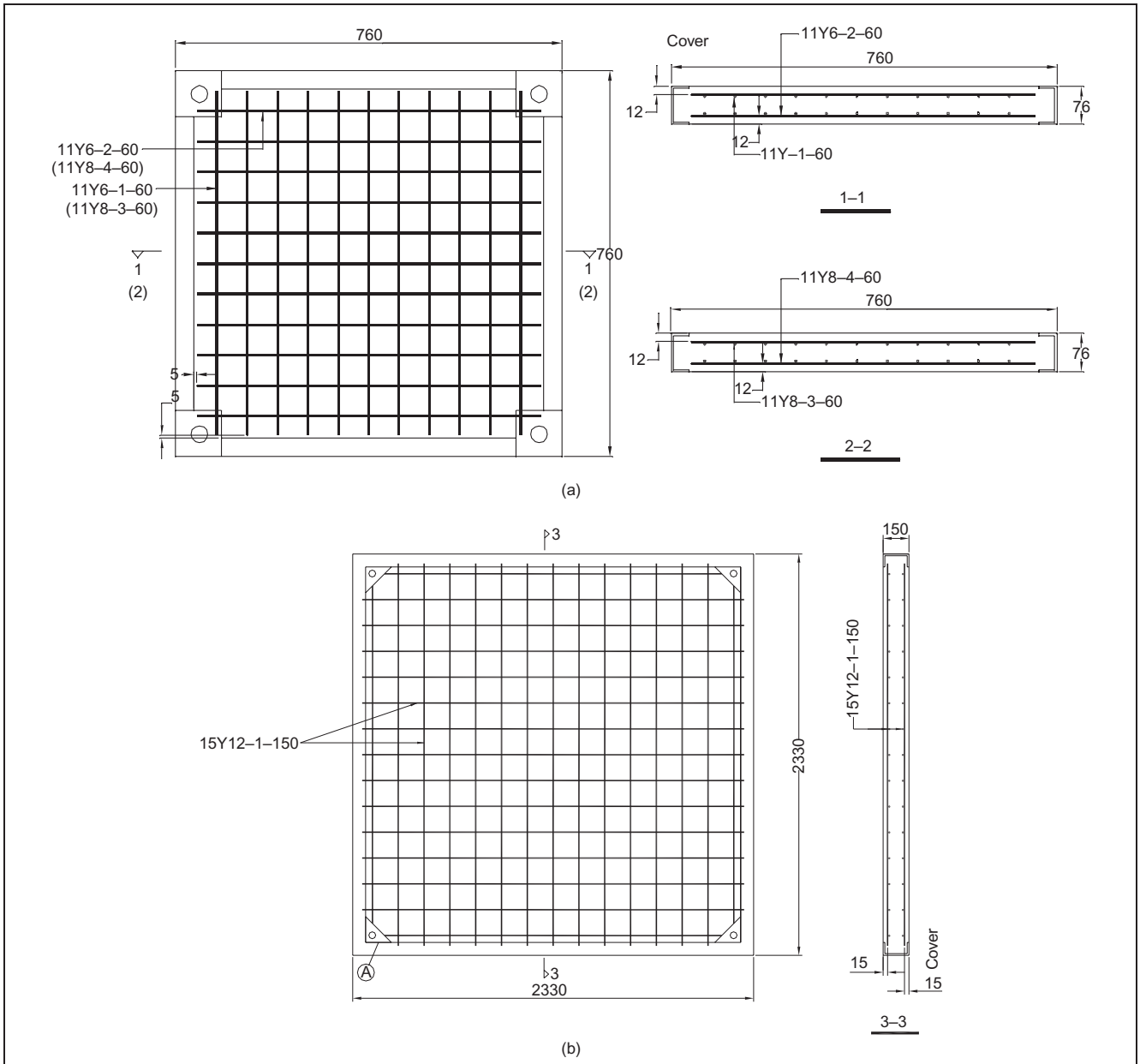

Figure 2. Details of slabs: (a) 0·76 m square slabs; (b) 2·3 m square slabs (dimensions in mm)

also help to gain further insights into the impact behaviour of reinforced concrete structures.

2. DESCRIPTION OF TESTS

2.1. Details of beams

The beams, were either 1·8 or 3·0 m long, of span 1·5 and 2·7 m respectively, reinforced with two 12 mm diameter high yield steel bars at the bottom and two 6 mm diameter mild steel bars at the top, 6 mm diameter mild steel shear links at 200 mm centres, and 25 mm concrete cover to the main steel. The tests on the beams were classified as type A and type B. Type A tests had a 12 mm thick plywood pad placed between a beam and the impactor, similar to some of the beams tested by Hughes and Speirs.[7] The results from the first few tests of type A beams were used to check the test procedure while also gathering additional data including video from the high-speed camera. Type B tests were used to investigate the effect of the impactor directly striking a beam. The details of the beam tests, including the dimension of the beams, the layout of the test and material properties can be found in Figure 1 and Table 1.

It was considered that, although strain rate could have some effect on the impact behaviour of beams and slabs, the influence would not be significant owing to the low impact speed. The dynamic properties of the materials were therefore not explicitly tested.

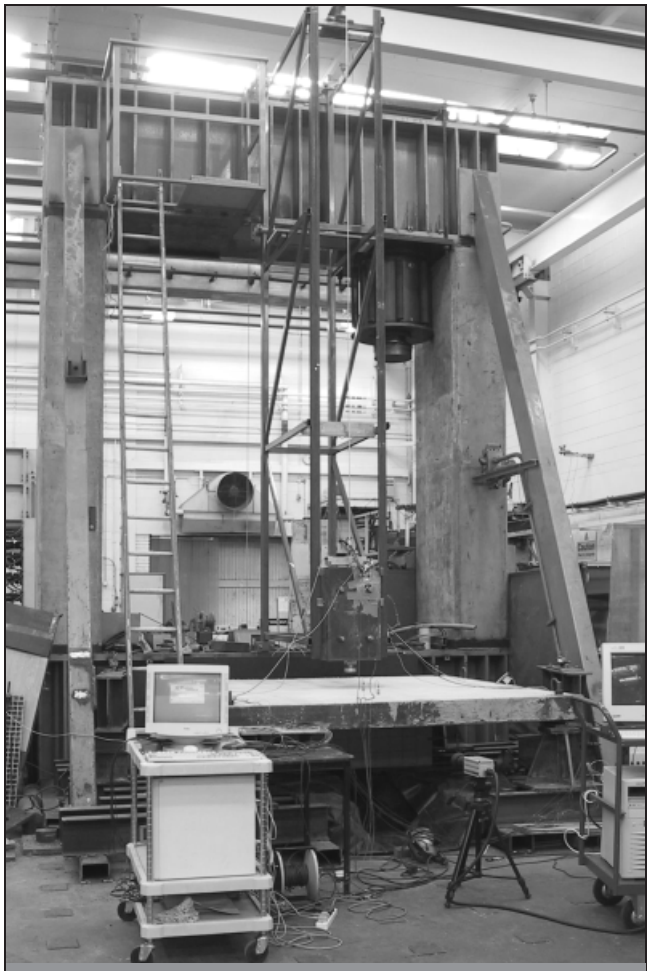

Figure 3. Drop-weight impact system

2.2. Details of slabs

Two sizes of slab were tested: 760 mm square and 76 mm thick, and 2320 mm square and 150 mm thick. Details are given in Table 2 and Figure 2.

2.3. Drop-weight impact system

The drop-weight system, as shown in Figure 3, can be used to test up to 3 m span beams and up to 2·4 m square slabs. A frame with two vertical steel angle legs was used to guide the striker, which can be raised up to 4 m high. The striker comprised a mass, a load cell and an impactor. The mass had two guides on each side, which were lined with acetal, a

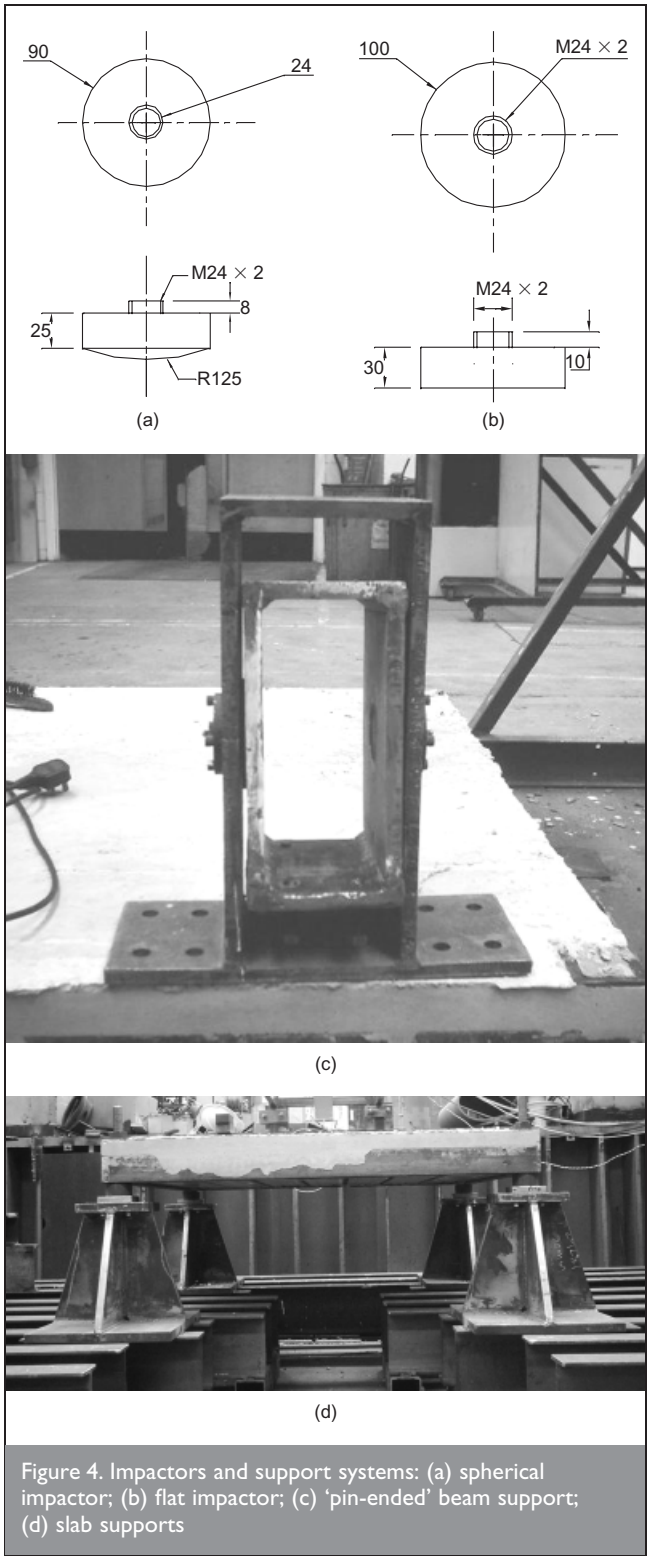

Figure 4. Impactors and support systems: (a) spherical impactor; (b) flat impactor; (c) 'pin-ended' beam support; (d) slab supports

thermoplastic material, in order to reduce the friction. The striker was lifted, using a winch, by a steel wire rope that is attached to the striker by an electromagnet. When the striker was at the required height it was released by switching off the magnet. To prevent an accidental release of the striker owing to a failure of the magnet, there was a mechanical link between the rope and striker, which was released prior to switching off the magnet.

Two types of impactors were used in the tests. The first was a stainless steel impactor with a 90 mm diameter and a hemispherical profile of 125 mm radius, the second was made of mild steel with a 100 mm diameter and a flat contact face (Figures 4(a) and (b)).

In the beam tests, a beam was either pin-ended or simply supported at the two ends. The 'pin-ended' supports, as shown in Figure 4(c), allowed rotation but were restrained axially and vertically by means of plates that clamped the beam. The supports were converted to 'simply supported' by releasing the clamps to allow horizontal movement and a small amount of upwards vertical movement, up to 50 mm, but no downward vertical movement.

The slabs were clamped at the four corners with both horizontal and vertical movement restrained (Figure 4(d)).

2.4. Instrumentation

The sensors that were employed to monitor the tests and provide high-quality data are outlined below.

(*a*) A high-speed video camera, Kodak HS Motion Analyzer, was used to record the impacts at a rate of 4500 frames per second with a resolution of 256 × 256 pixels. Higher rates could be used, but with a reduced resolution. The camera had a memory of 3 GB with which a total of approximately 40 000 frames of image could be recorded. The images recorded by the camera were initially stored in the camera's memory and then transferred to the hard drive of a computer.

(*b*) In most tests the impact forces were measured using a load cell, which was placed between the mass and the impactor. For tests where the impact load was expected to exceed the capacity of the load cell, the impact force was derived from accelerometers installed on the striker.

(*c*) Acceleration at various points on a beam or slab was measured using accelerometers. To reduce noise, the results from accelerometers were filtered with a Butterworth filter with a cut-off frequency of 2000 Hz.

(*d*) In some of the tests, the reinforcement had strain gauges placed inside the bar, using a technique developed by Scott and Marchand.[20] By this measure the strains in the reinforcement could be recorded without affecting the bond between the reinforcement and surrounding concrete.

(*e*) Two electronic triggers spaced at 40 mm at the bottom of the guiding legs of the frame measured the velocity of the striker at the moment of impact. An additional trigger was used to enable recording of the transducers and high-speed video camera to commence simultaneously.

The outputs of the load cell, accelerometers and strain gauges were amplified and then fed into an A/D data acquisition computer module at a sequential sampling rate of 500 kHz.

In all the tests, the striker was unrestrained vertically so that after the first impact it rebounded and then fell to impact the specimen again. The deformation of the structure member and propagation of cracks could thus further

Group no.	Test no.	F_m: kN	F_{AVG}: kN	$(F_m - F_{AVG})/F_{AVG}$: %	t_m: ms	t_{AVG}: ms	$(t_m - t_{AVG})/t_{AVG}$: %	Failure type
A1	1	n/a	230	n/a	n/a	1·8	n/a	a
	2	223		−3·0	2·1		+16·7	a
	3	234		+1·7	1·5		−16·7	a
	4	233		+1·3	2·0		+11·1	a
	5	n/a		n/a	n/a		n/a	a
	6	229		−0·4	1·4		−22·2	a
A1*	7	128	—	—	1·6	—	—	a
A2	8	214	222	−3·6	2·0	1·8	+11·1	a
	9	230		+3·6	1·6		−11·1	a
A3	10	194	—	—	2·0	—	—	a
B1	11	n/a	—	n/a	n/a	—	n/a	b
	12	161		—	1·3		—	b
B1*	13	183	—	—	1·4	—	—	b
B2	14	169	170	−0·6	1·5	—	0	b
	15	171		+0·6	1·5	—	0	b, c
B3	16	654	—	—	0·3	—	—	c
B3*	17	215	—	—	1·0	—	—	c
B4	18	241	—	—	1·0	—	—	c

Notes:
F_m: maximum impact force.
t_m: time of maximum impact force (peak time).
Result not available owing to instrument failure.
Failure: type a—flexural failure and no spalling of impact zone; type b—highly yielding or rupture of tension steel, spalling of impact zone; type c—scabbing and spalling.

Table 3. Maximum impact force, peak time and failure type of beam tests

develop under subsequent strikes. The response of the specimen under these strikes was, however, not as significant as under the first impact. In the present paper only the behaviour of the member under the first impact, which lasted for about 50 ms for the beams and 20–30 ms for the slabs, is examined.

3. BEAM RESULTS

3.1. Repeatability

Table 3 lists the maximum impact forces, peak times, the time at which the maximum impact force occurred, and failure modes of the beams.

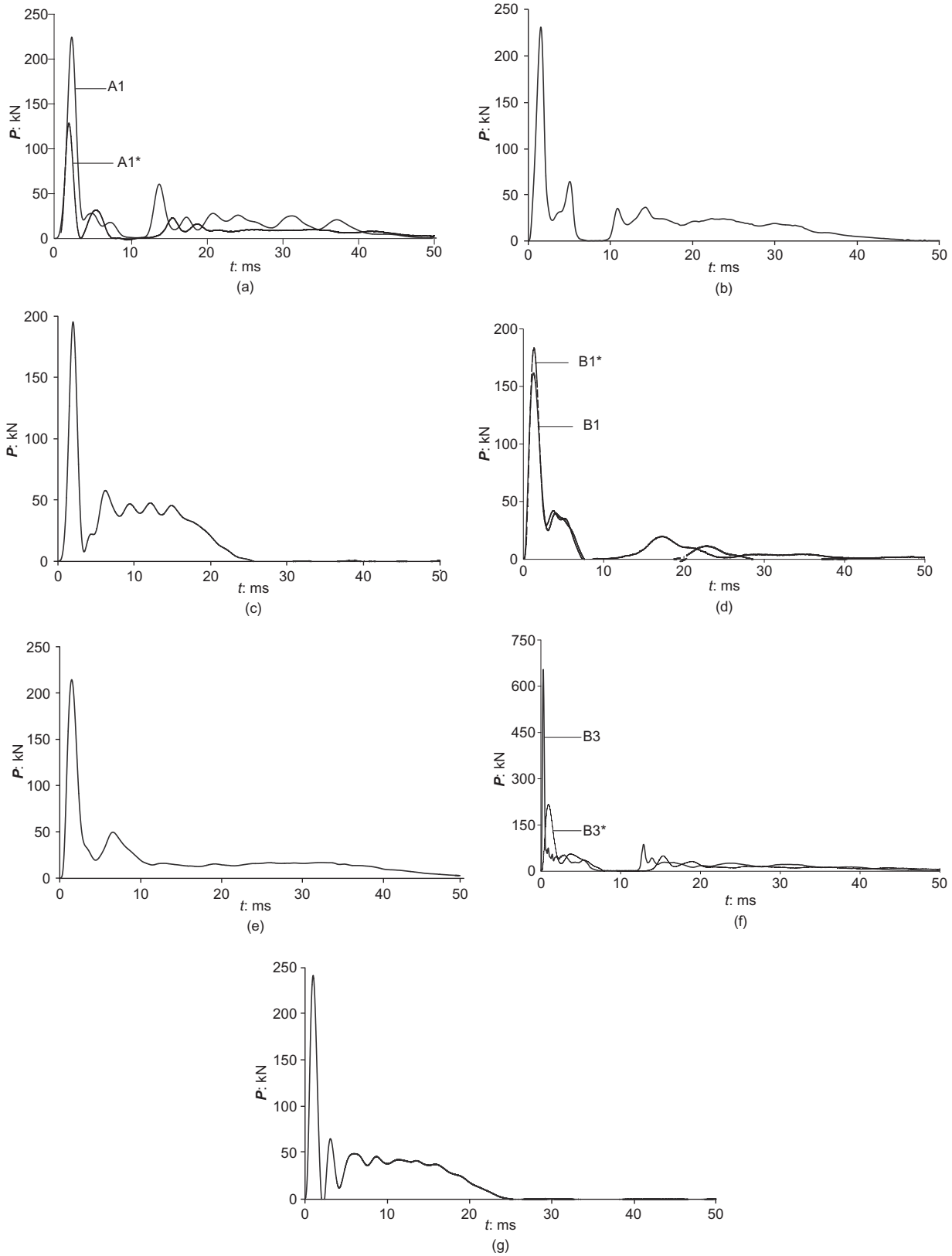

Figure 5. Transient impact load of beams: (a) beam A1(A1*); (b) beam A2; (c) beam A3; (d) beam B1(B1*); (e) beam B2; (f) beam B3(B3*); (g) beam B4

Seven A1 beams were tested to assess the repeatability of tests and to give an indication of scatter. The transient responses of these beams were found to be remarkably similar to each other and the failure patterns were the same.

For seven A1 beams, the average maximum impact force was 230 kN with a variation of up to 3%, and the average peak time was 1·8 ms with a variation of up to 22%. A beam similar to beam A1 failed at less than 20 kN under static loading.[7]

There were repeat tests of beams A2, B1 and B2, the results of which were similar to the initial tests.

3.2. Transient impact forces

Figure 5 shows typical impact load–time histories for a number of beams. Comparing Figure 5(a) for beam A1, which was pin-ended, and Figure 5(b) for beam A2, which was simply supported, both of 2·7 m span, it is found that the load–time histories are very similar. It would therefore appear that the end conditions have little effect on the impact response of the beams; however, the impact force is dependent on the span of a beam. This finding is similar to that noted elsewhere.[7]

The plywood interface, the properties of which are given by Hughes and Speirs,[7] and the flat impactor appear to have distributed the impact force in a similar way. Thus the impact load–time histories of, for example, beam A3, which had a 12 mm thick plywood section between the impactor and the beam, and beam B4, which was struck directly by a flat impactor, are similar.

It is difficult to draw any conclusion regarding concrete strength on the peak load. For example, a comparison between beam A1* and the set of beams A1 shows that, while the concrete strength is about 30% less, the peak load is 45% less. Similarly for beams B1 and B1* the ratios are 27% and 13% less and for B3* and B3 30% and 70%. This is an area that requires further investigation.

3.3. Transient accelerations

Figure 6 shows the acceleration–time histories from the records of accelerometers attached to the top of beam A2.

3.4. Transient reinforcement strains

The strains in the steel reinforcement in the bottom of a beam were measured in a number of tests. Figure 7 shows the reinforcement strain–time history for beam B3. The yield strain of the reinforcement was of the order of 3000 $\mu\varepsilon$ and thus it can be seen that generally the reinforcement had yielded during the initial impact.

The maximum strain rate recorded in the tests was 32·5/s.

3.5. High-speed camera recording

A high-speed camera was used to record the local response of the beams in the impact zone throughout the loading. Typical video footage generated from the images captured by the camera is available.[21]

3.6. Correlation between transient load and beam crack development

Figures 8 and 9 show the impact load–time histories, together with a number of images taken from the camera, to show the crack development adjacent to the impact zone for beam A1 and beam B3, respectively.

Figure 8 shows that, initially a group of diagonal shear cracks formed on beam A1 as the load reached its maximum at 2 ms. This was followed by the development of vertical flexural cracks. Separation between the impactor and beam occurred at about 10 ms, which is indicated by zero impact load, though both the beam and striker continued to move downwards. At this time some spallation of the concrete can be observed directly beneath the impactor. The impactor and beam then regained contact, more cracking occurred and the spallation became more apparent. At 50 ms the beam and impactor separated again as the latter started to move upwards.

In Figure 9 it can be seen, however, that there was virtually no cracking on beam B3 before the impact force reached its maximum at 0·3 ms. Two major diagonal shear cracks formed symmetrically about mid-span beneath the impact zone at about 0·5 ms, together with some minor vertical flexural cracks at the bottom and in the central part of the beam. Further,

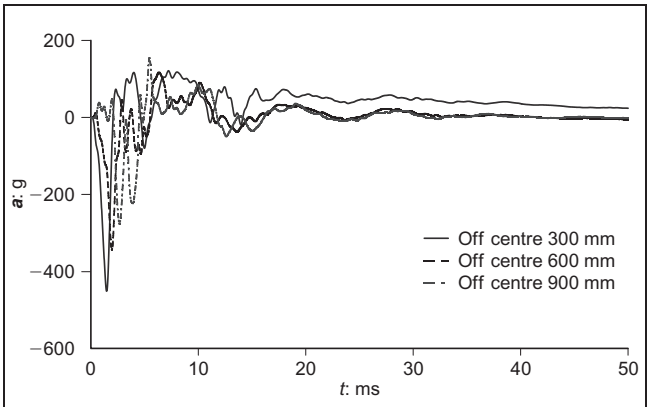

Figure 6. Transient acceleration of beam A2

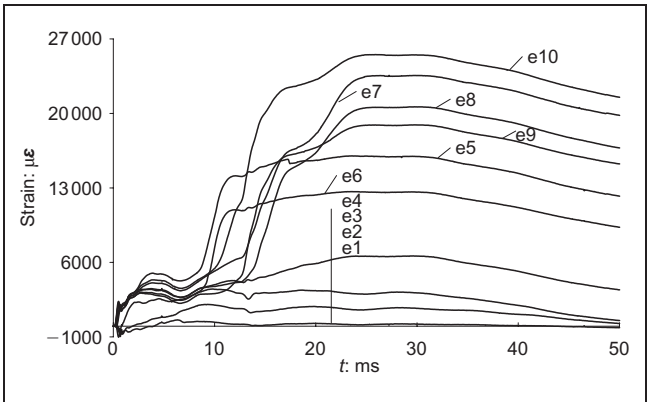

Strain gauge no.	e1	e2	e3	e4	e5	e6	e7	e8	e9	e10
Distance from mid-span: mm	890	665	440	190	140	115	65	40	15	10

Figure 7. Transient reinforcement strain measurement for beam B3

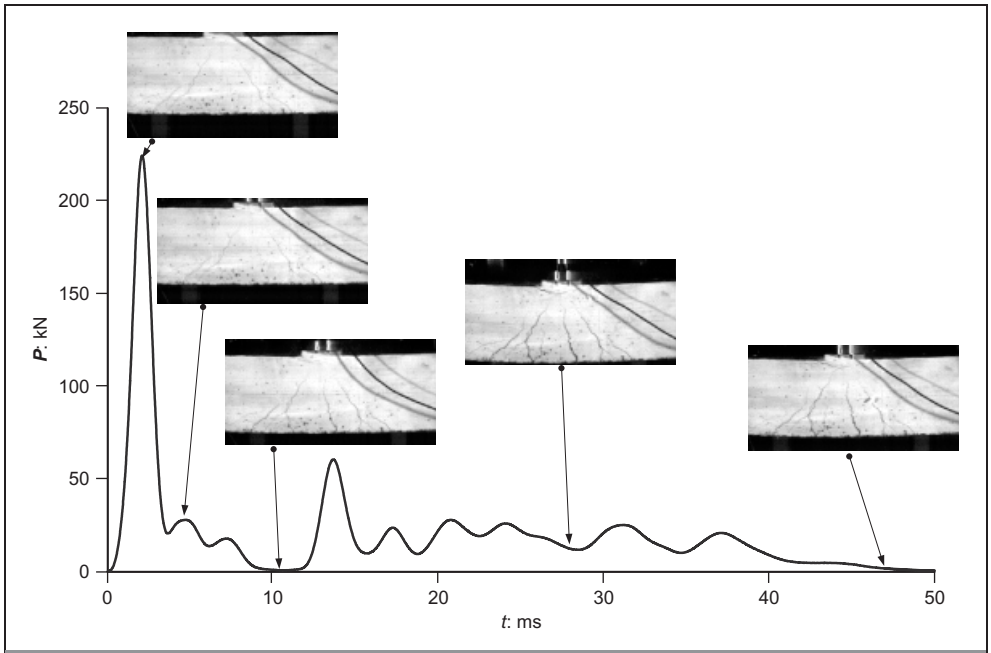

Figure 8. Correlation between impact load and crack propagation for beam A1

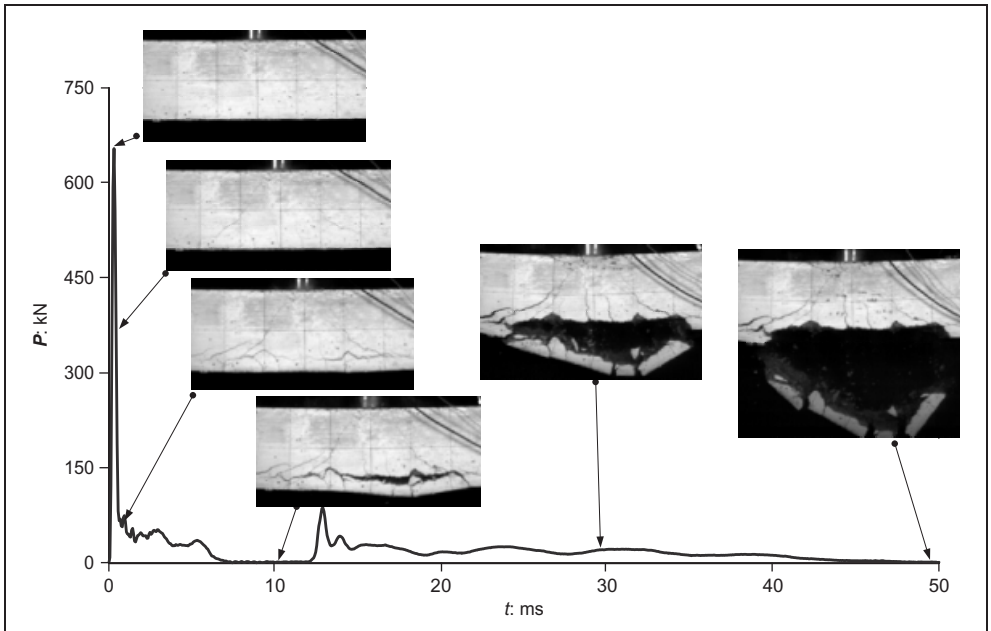

Figure 9. Correlation between impact load and crack propagation for beam B3

different to beam A1, a number of horizontal cracks were observed at the level of the bottom steel reinforcement below the impact zone. They subsequently joined to become one crack as the time increased while the load decreased. A short period of separation between the impactor and beam occurred as the beam deformed at a faster rate than the impactor at around 8 ms. The opening of the horizontal crack became so large that the concrete cover below the crack started to separate, or scab, from the rest of the beam. From 10 ms to 30 ms the impactor and beam contacted again leading to a relatively small impact load. Spallation also occurred during this period beneath the impact zone. The scabbing of the concrete became more significant between 30 and 50 ms. Finally a substantial amount of the concrete cover at the bottom of the beam broke off from a triangular region enclosed by the two diagonal shear cracks. At about 50 ms the striker started to move upwards and the beam and impactor separated again.

3.7. Post-test crack patterns or failure modes

Three modes of failure were observed.

Mode a. This was a predominantly flexural failure with some crushing beneath the impactor and some shear cracking in the impact zone. Vertical cracks starting from the top of a beam were found along the beam section away from the impact zone, as shown in Figures 10(a) and 10(b) for beams A1 and A2 respectively. Further shear cracking and short vertical cracking occurred in beam A3, as shown in Figure 10(c). Mode a failure occurred on type A beams, namely those with the plywood interface. There was less damage in this type of failure than in modes b and c, described below, owing to some of the impact energy being absorbed in deforming the plywood.

Mode b. This was a mainly localised failure at the impact zone with extensive concrete crushing below the impactor, and yielding of the tension steel bars, as shown in Figures 10(d) and 10(e) for beams B1 and B2 respectively. Away from the impact zone the cracking was similar to that of mode a failure. This mode of failure occurred on beams impacted directly with the hemispherical impactor.

Mode c. This was similar to mode a failure, but was accompanied by loss of the concrete cover to the tension steel reinforcement at the bottom of a beam owing to scabbing, as shown in Figures 10(f) and 10(g) for beams B3 and B4 respectively. It occurred on beams impacted directly with the flat impactor.

4. SLAB RESULTS

4.1. Transient impact load

The striker for slab 1 comprised the hemispherical impactor and mass but no load cell. The test was carried out to

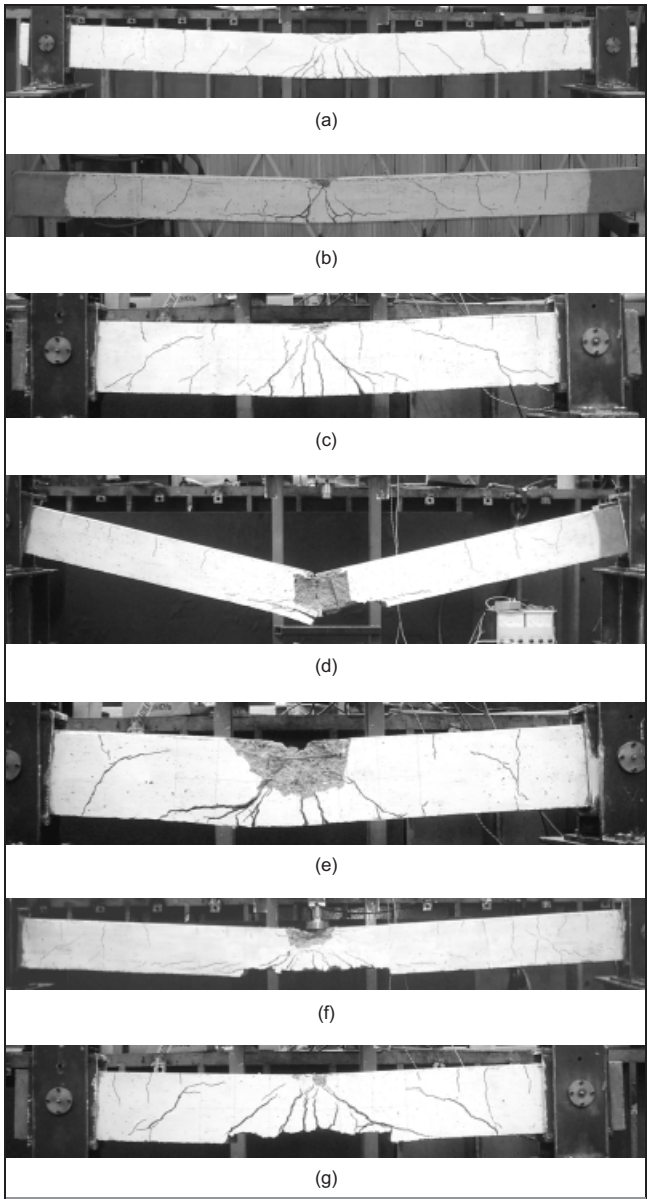

Figure 10. Post-test crack pattern of beams: (a) beam A1; (b) beam A2; (c) beam A3; (d) beam B1; (e) beam B2; (f) beam B3; (g) beam B4

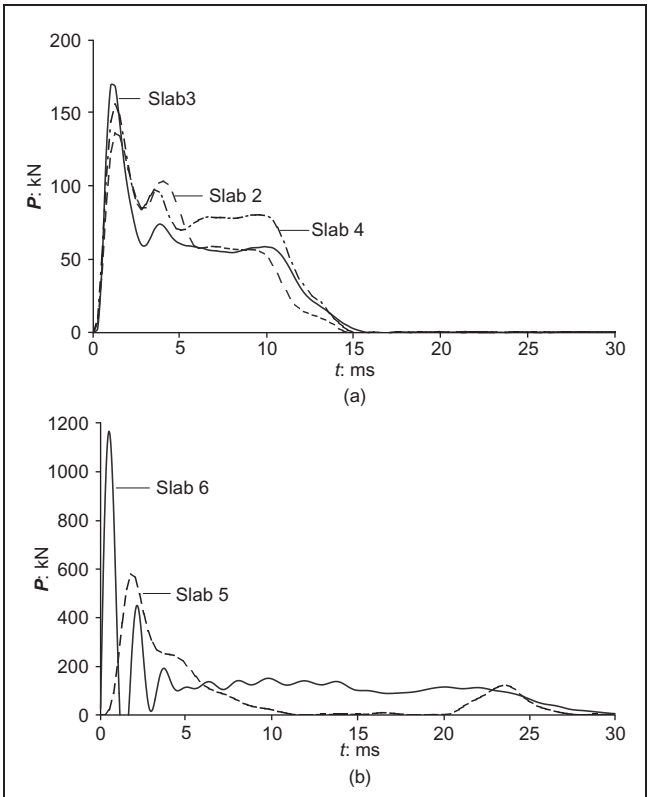

Figure 11. Transient impact load of slabs: (a) slab 2–4; (b) slabs 5 and 6

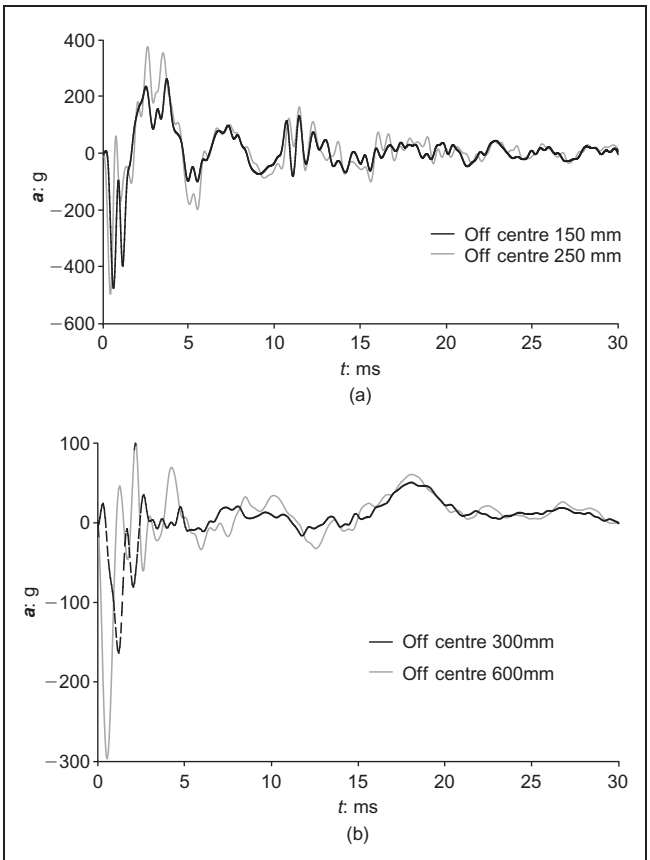

Figure 12. Transient acceleration of slabs: (a) slab 4; (b) slab 6

establish if perforation of the slab would occur, which could have led to damage to the load cell if it had been installed. Thus there was no record of the impact load for slab 1. Figure 11 shows the impact load–time histories for slabs 2 to 6. For slabs 2 to 5, the loads were measured using the load cell. For slab 6, the load was determined from the accelerations measured by an accelerometer attached to the dropping mass, because the impact load exceeded the capacity of the load cell.

From Figure 11(a) it is seen that for slabs 2 to 4 after reaching the peak load the load fell until it arrived at a plateau of approximately half of the peak load. In slab 6 the magnitude of the plateau load is about one-ninth of the peak load, in slab 5 the plateau is absent. During this time local failures owing to penetration and scabbing, accompanied by yielding of the reinforcement, were observed to various degrees in slabs 2 to 4 and 6. Slab 5 shows little signs of failure, as will be discussed later.

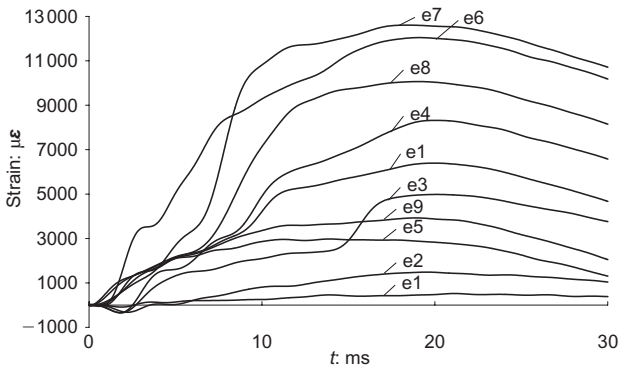

Strain gauge no.	e1	e2	e3	e4	e5	e6	e7	e8	e9	e10
Distance from mid-span: mm	900	675	450	450	200	150	125	120	50	0

Note: strain gauges with same distance away from the centre were placed opposite of the centre.

Figure 13. Transient reinforcement strain in slab 6

4.2. Transient accelerations

The transient accelerations measured on the top surfaces of slabs 4 and 6 are shown in Figures 12(a) and 12(b), respectively. There is little difference between the phases of the two accelerations measured at different points on slab 4. On slab 6, the difference in the phases of the accelerations is more evident for the first 5 ms but reduces as time increases. On slabs 5 and 6 the accelerometers were placed further apart than those on 0·76 m square slabs and it is considered that the difference in the phases of the accelerations reflects the lag in response of the various parts of the 2·3 m square slabs owing to the wider spacing.

4.3. Transient reinforcement strains

The strains in the reinforcement in slab 6 were also measured and the results are shown in Figure 13. The strains indicate that some of the reinforcement yielded during the test.

4.4. Local damage and comparison with empirical formulae

Figure 14 shows the damage, after the impact, to the top and bottom faces of the slabs. On the 76 mm thick slabs 1 to 4 there was a larger amount of concrete debris, in the form of both small particles and larger blocks, ejected owing to scabbing than on the 150 mm thick slabs. This was due to the proportionally more significant amount of energy in the impacts on the thinner slabs. There was also some scabbing on slab 6, but on the other thick slab, slab 5, in which the mass of the impactor was approximately half that for slab 6, scabbing was not fully developed. There was also a significant amount of penetration of the impactor in slabs 1 to 4 and 6 but very little in slab 5.

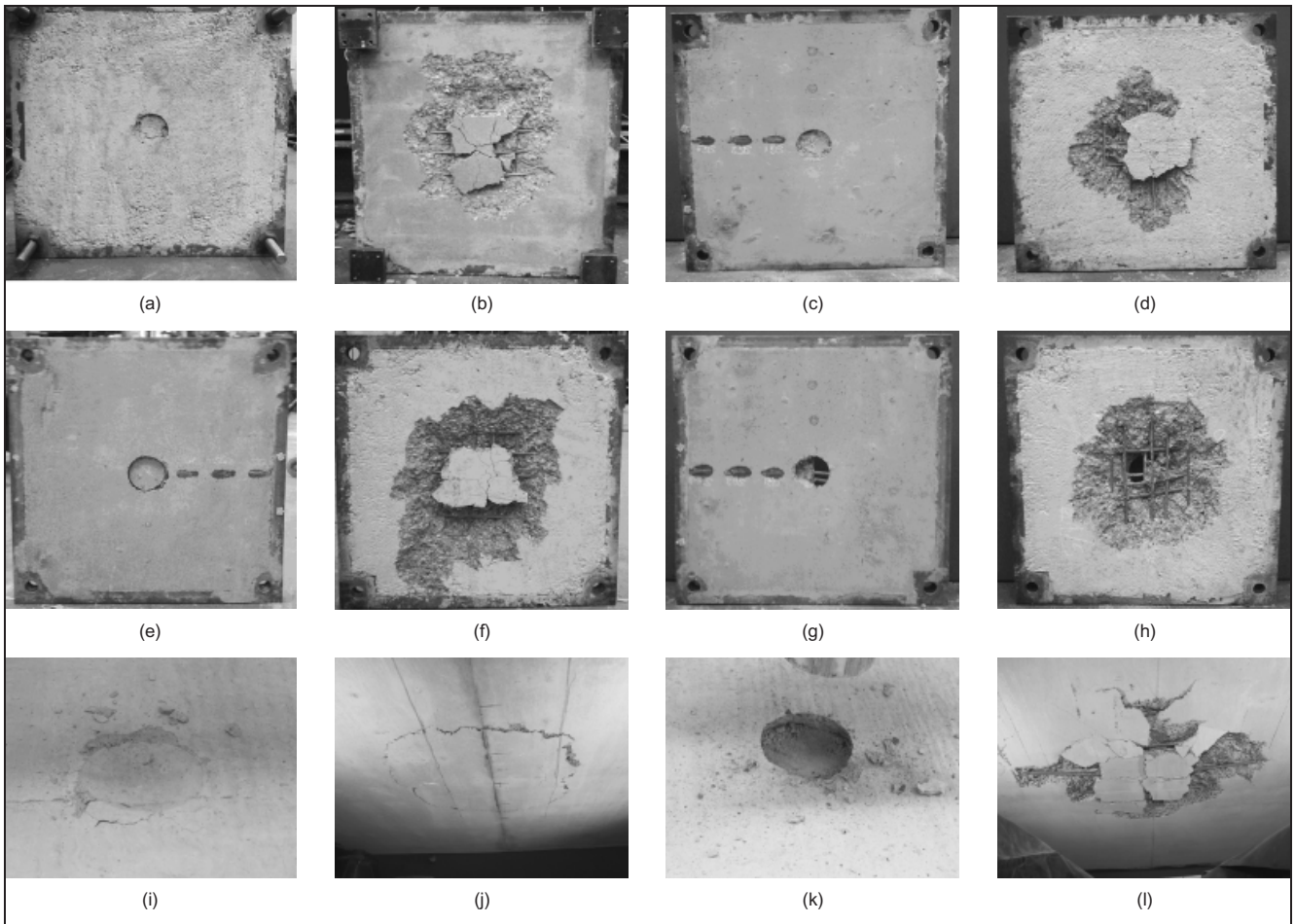

Figure 14. Slabs after impact: (a) top face of slab 1; (b) bottom face of slab; (c) top face of slab 2; (d) bottom face of slab 2; (e) top face of slab 3; (f) bottom face of slab 3; (g) top face of slab 4; (h) bottom face of slab 4; (i) top face of slab 5; (i) bottom face of slab 5; (k) top face of slab 6 ; (l) bottom face of slab 6

Slab no.	Impact energy E_{imp}: kJ	Diameter of scabbing zone: mm	Mass of scabbed concrete: kg	Slab thickness to prevent scabbing			Slab thickness to prevent perforation		Energy of scabbing	E_{imp}/E_s
				Modified NDRC formula:[14] mm	Bechtel formula:[14] mm	Stone and Webster formula:[14] mm	Modified NDRC:[14] mm	CEAS-EDF formula:[14] mm	BNFL E_s:[22] kJ	
1	2·1	450–480	2·9	130	146	110	58	55	2·2	0·97
2	2·1	360–480	2·9	130	146	110	58	55	2·2	0·97
3	2·1	410–620	5·1	119	143	113	52	52	2·7	0·76
4	3·2	410–430	5·6	152	162	126	69	64	3·4	0·93
5	7·5	—	—	217	251	174	108	106	5·3	1·42
6	13·0	~700	—	249	293	209	133	132	5·8	2·25

Table 4. Details of scabbing (NDRC: National Defence Research Committee)

Table 4 gives the size of scabbing zones and the weight of ejected debris for the slabs. Using a hemispherical impactor was found to create a more circular scabbing zone on the bottom face of a slab than that caused by a flat impactor as used on slab 3. This is because the stress wave caused by the hemispherical impactor may have propagated more uniformly owing to the progressive contact between the impactor and the top face of the slab.

Together with test results, Table 4 also gives predictions related to scabbing using various empirical formulae. The predictions are the minimum thickness of a slab to prevent either scabbing or perforation and the minimum impact energy required to cause scabbing. For example, for a 98·7 kg mass with a velocity of 6·5 m/s impacting a slab similar to slab 1 with a compressive strength of concrete at 60 N/mm^2, the modified NDRC formula[14] predicts that perforation would occur if the thickness were less that 58 mm and scabbing would occur for thicknesses less than 130 mm. The impact energy needed to cause scabbing of a 76 mm thick slab is 2·2 kJ, based on British Nuclear Fuels (BNFL) formula.[22]

A comparison of the test results with the predictions suggests that empirical formulae work well for slabs 1 to 4. It is found that the thickness of the slabs, 76 mm, falls in the range of slab thicknesses predicted for scabbing, and scabbing did occur when the impact energies close to those predicted were deployed in the tests. For slabs 5 and 6, the formulae seem not do as well as for 76 mm thick slabs. For example, little scabbing was observed in the tests, even though the impact energy used in the tests was greater than that predicted using the BNFL formula for scabbing,

The video footage is also available for the slab tests.[21] In general, however, the video footage obtained was considered not to be as useful as that obtained in the beam tests.

5. CONCLUSIONS

An experimental investigation into the behaviour of reinforced concrete beams and slabs under high-mass low-velocity impact loads has been described. Transient measurements of impact force, accelerations on the beams and slabs, and the strain of reinforcement have been presented. The beam tests have confirmed the findings of others[7] that beam supports have less influence on the impact force than the span. It has also been found that the plywood interface, which was used in some tests, distributes the force in a similar form to a flat impactor. The records from the high-speed camera have enabled the impact response of the beams in terms of cracking, scabbing and spallation to be correlated against the load-time histories. A comparison of the impact energy deployed on the slabs and that predicted using the empirical formulae shows that the formulae were unable to give an accurate prediction for the 150 mm thick slabs though the predictions were satisfactory for the 76 mm thick slabs under high-mass low-velocity impacts. Some of the data produced from this study have already been used to calibrate numerical procedures for the simulation of impact-loaded reinforced concrete structures and further use can be expected.

ACKNOWLEDGEMENT

The support of the Engineering and Physical Sciences Research Council (EPSRC) is gratefully acknowledged.

REFERENCES

1. FARAH A. Structural serviceability under impact and dynamic loadings. *Proceedings of Structures under Shock and Impact*, New Forest, 2006, pp. 467–474.
2. JOHNSON G. R. and COOK W. H. A constitutive model and data for metals subjected to large strains, high strain rates and high temperatures. *Proceedings of the 7th International Symposium on Ballistics, The Hague*, 1983, 541–547.
3. BISCHOFF-PERRY M. and RILEM S. *Concrete Structures Under Impact and Impulsive Loading: Synthesis Report*. CEB-187, 1988.
4. BRARA A., CAMBORDE F., KLEPACZKO J. R. and MARIOTTI C. Experimental and numerical study of concrete at high strain rates in tension. *Mechanics of Materials*, 2001, **33**, No. 1, 33–45.
5. KISHI N., MIKAMI H., MATSUOKA K. G. and ANDO T. An empirical impact resistant design formula of RC beams with statically bending failure mode. *Japanese Society of Civil Engineers*, 2000, **647**, No. I–51, 177–190 (in Japanese).
6. KISHI N., MIKAMI H., MATSUOKA K. G. and ANDO T. Impact behaviour of shear-failure-type RC beam without shear rebar. *International Journal of Impact Engineering*, 2002, **27**, No. 9, 955–968.
7. HUGHES G. and SPEIRS D. M. *An Investigation of the*

Beam Impact Problem. C&CA UK, 1982, Technical Report 546.
8. AGARDH L., MAGNUSSON J. and HANSSON H. *High Strength Concrete Beams Subjected to Impact Loading, an Experimental Study*. Defence Research Establishment (FOA), Tumba, Sweden, 1999, FOA-99-01187-311-SE.
9. BARR P., CARTER P. G., HOWE W. D. and NEILSON A. J. Replica scaling studies on hard missile impacts on reinforced concrete. *Proceedings of CEB International Symposium on Concrete Structures under Impact and Impulsive Loading,* Berlin, 1982, pp. 329–344.
10. DANCYGIER A. N. Effect of reinforcement ratio on the resistance of reinforced concrete to hard projectile impact. *Nuclear Engineering and Design*, 1997, **172**, No. 1-2, 233–245.
11. KISHI N., MATSUOKA K. G., MIKAMI H. and GOTO Y. Impact resistance of large scale RC slabs. *Proceedings of the 2nd Asia–Pacific Conference on Shock Impact Loads on Structures, Melbourne*, 1997, 213–220.
12. TSUBOTA H., MIZUNO J., KUSAMA K. and MOMMA T. Experimental studies on the inelastic behaviour of reinforced concrete panels under high-speed loadings, Part 1. Effects of dynamic loading. *Proceedings of the 5th International Conference on Structures Under Shock and Impact. Thessolaniki, Greece*, 1998, 743–758.
13. BROWN I. C. and PERRY S. H. Development of a new assessment method, Part B. In *Assessment of Impact Damage Caused by Dropped Objects on Concrete Offshore Structures*. HMSO, London, 1989, pp. 79–151.
14. SLITER G. E. Assessment of empirical concrete formulas. *Journal of the Structural Division, ASCE*, 1980, **106**, No. ST5, 1023–1045.
15. ANDO T., KISHI N., MATSUOKA K. G. and MIKAMI H. FEM analysis on RC beams under impact loading. *Proceedings of the 3rd Asia–Pacific Conference on Shock and Impact Loads on Structures, Singapore*, 1999, 51–56.
16. ISHIKAWA N., KATSUKI S. and TAKEMOTO K. Impact failure analysis of prestressed concrete beams using RBSM–FEM combined model. *Proceeding of the 4th Asia–Pacific Conference on Shock and Impact Loads on Structures, Singapore*, 2001, 27–37.
17. UNOSSON M. Numerical simulations of the response of reinforced concrete beams subjected to heavy drop tests. *Impact Engineering and Application: Proceedings of the 4th International Symposium on Impact Engineering, Kumamoto, Japan*, 2001, 613–618.
18. AGARDH L. and LAINE L. 3D FE-simulation of high-velocity fragment perforation of reinforced concrete slabs. *International Journal of Impact Engineering*, 1999, **22**, No. 9–10, 911–922
19. MAY I. M., CHEN Y., OWEN D. R. J., FENG Y. T. and THIELE P. J. Reinforced concrete beams under drop-weight impact loads. *Computers and Concrete*, 2006, **3**, No. 2/3, 79–90.
20. SCOTT R. H. and MARCHAND K. A. Measurement of reinforcement strains caused by blast loading. *Strain*, 2000, **36**, No. 4, 161–164.
21. Impact testing. See: http://www.sbe.hw.ac.uk/research/structural/impact_test/index.htm. Accessed 10/12/2006.
22. BRITISH NUCLEAR FUELS. Appendix H, *Reinforced Concrete Slab Local Damage Assessment*. BNFL Commercial, 2003, R3 Procedure, Vol. 3.